Temperature Estimates of Lower Miocene (Burdigalian) Coastal Water of Southern India Using a Revised Otolith "Clumped" Isotope Paleothermometer

K. Prasanna[1,2,3], Prosenjit Ghosh[2,3], Robert A. Eagle[4], Aradhna Tripati[4], Vivesh V. Kapur[1], Richard F. Feeney[5,†], Benjamin R. Fosu[2], and Divya Mishra[2]

[1]Birbal Sahni Institute of Palaeosciences, Lucknow, India, [2]Centre for Earth Sciences, Indian Institute of Science, Bangalore, India, [3]Divecha Centre for Climate Change, Indian Institute of Science, Bangalore, India, [4]Department of Earth, Planetary, and Space Sciences, Department of Atmospheric and Oceanic Sciences, Institute of the Environment and Sustainability, Center for Diverse Leadership in Science, University of California, Los Angeles, CA, USA, [5]Natural History Museum of Los Angeles County, Los Angeles, CA, USA

Abstract Carbonate clumped isotope thermometry is based on the ordering of ^{13}C and ^{18}O in the carbonate lattice and is based on the relative abundance of $^{13}C^{18}O^{16}O$ in CO_2 produced through acid digestion of carbonate minerals. The major advantage of this technique is its non-dependency on the $\delta^{18}O$ value of water from which the carbonate precipitated. Ghosh et al. (2007, https://doi.org/10.1016/j.gca.2007.03.015) previously published calibration data for fish otoliths referenced to heated gases and used the Gonfiantini ^{17}O parameter set in their data evaluation. Herein, we present a new clumped isotope (Δ_{47}) calibration for aragonitic fish otoliths in the absolute reference frame using the International Union of Pure and Applied Chemistry ^{17}O correction. Our revised calibration equation for otolith is:

$$\Delta_{47\,CDES} = 0.0364 \pm 0.005 \times \frac{\left(10^6\right)}{T^2} + 0.2619 \pm 0.0657 \left(R^2 = 0.9, p-\text{value} < 0.001\right).$$ To test the accuracy of this calibration, we apply it to otoliths of modern *Lutjanus lutjanus* from the Bay of Bengal. The estimated average temperature ($22.3°C \pm 4.2°C$) for the Bay of Bengal and $\delta^{18}O_{V\text{-SMOW}}$ composition of waters of $-1.7‰$ (± 0.5) are consistent with the onsite observations. We also apply the new calibration to well-preserved otoliths of "genus Ambassidarum" sp. and "genus Gobiidarum" sp. from lower Miocene (Burdigalian) sediments of the Quilon Formation, India to quantify coastal water conditions. Estimated average environmental water temperatures in their habitats were $12.9°C \pm 1.7°C$, and the average $\delta^{18}O_{V\text{-SMOW}}$ of ambient waters calculated yielded a value between $-3.5‰$ and $-2.6‰$ (V-SMOW) (mean: $-2.9‰ \pm 0.4$) and $-4.4‰$, respectively. These results indicate $\delta^{18}O$ values reflect the kinetic effects impacting the $\delta^{18}O$ of fish otoliths independently of Δ_{47}, although we cannot fully preclude diagenesis.

1. Introduction

Otoliths are accretionary body parts deposited within the inner ear of fishes. They accrete new crystalline and protein material onto their exterior surface daily. Incorporated within these accreted layers are minor and trace elements along with the aragonitic mineralization. Because the majority of fishes are ectothermic, meaning they do not have physiological mechanisms to regulate their body temperature, these accretionary body parts deposited within the inner ear of fishes are used as recorders of the environment and are thus, an essential archive for paleo-climatic studies (Thorrold et al., 1997). Assuming fish otoliths form under equilibrium conditions, their stable isotope ratios of carbon ($\delta^{13}C$) and oxygen ($\delta^{18}O$) may therefore be used for the estimation of temperatures of their habitats (Fay, 1984; Morris & Kittleman, 1967). Being monomineralic (aragonitic), they can be screened for diagenetic effects based on the determination of the occurrence of secondary calcite using bulk mineralogical analyses (such as XRD or FTIR) and assessment of the degree of local structural ordering using micro Raman techniques (Toffolo, 2021). Previous studies employing the $\delta^{18}O$ composition of otoliths demonstrated that the accretionary growth layers is in equilibrium with the water in which the host fish lives (Kalish, 1991b; Patterson et al., 2013; Thorrold et al., 1997). This equilibrium relationship has been applied to track environmental temperatures and migration routes for species of modern fish, constrained by the water $\delta^{18}O$ value (Campana & Neilson, 1985).

A significant limitation of $\delta^{18}O$ based paleo-environment reconstruction is partitioning of this combined signature of temperature and water isotopes into meaningful climatic signals. The application of carbonate $\delta^{18}O$ in reconstructing paleo-environments suffers from limited constraints on the isotopic composition of paleo-environmental waters. This is because the equilibrium formation of aragonite in otoliths, with respect to oxygen isotopic composition, depends on the isotopic composition and temperature of the water. Thus, an assumption of either the isotopic composition or temperature of the water is required to determine the other when using conventional oxygen isotope thermometry. This limitation may be circumvented with the "carbonate clumped isotope thermometer" (Eiler, 2011; Ghosh et al., 2006; Schauble et al., 2006). A significant advantage of using this isotope geothermometer is that it relies on a homogeneous equilibrium (reaction among components of a single phase). Therefore, it can rigorously constrain the temperature of carbonate growth without any prior knowledge of the isotopic composition of its parent water.

The foundation of this thermometer was the empirical relationship established by analyzing calcite precipitated at controlled temperatures ranging between 5°C and 50°C, reported on a stochastic reference frame derived by analyzing CO_2 heated to 1,000°C (Ghosh et al., 2006). The early empirical calibration for the carbonate clumped isotope thermometer was applied to biogenic corals from deep and surface ocean locations with known growth temperatures (Ghosh et al., 2006). The calibrations was later extended to otolith specimens from modern fishes sampled across the latitudinal transect of the Atlantic Ocean (between 54°S and 65°N), and other species from the tropical western Pacific (Ghosh et al., 2007) with growth temperatures varying between 2°C and 25°C. These observations showed that the Δ_{47} values of otoliths varied with growth temperature, making it a potential archive for paleo-climate reconstruction. Since these early studies, the clumped isotope proxy has been applied to various geological archives and there have been significant advances in calibrations, analytical developments, standardization, and data reduction efforts (Bernasconi et al., 2021; Daëron, 2021; Daëron et al., 2016; Dennis et al., 2011; Fernandez et al., 2017; Kelson et al., 2017; Meckler et al., 2014; Petersen et al., 2019; Saenger et al., 2021). These advances were necessary because of discrepancies in Δ_{47}-temperature (T) calibrations and Δ_{47} data acquisition regimes. Improvements have since been made in temperature (Δ_{47}-T) calibrations and overall Δ_{47} data evaluation but important discrepancies remain and are thought to relate to methodological differences among laboratories, for example, sample preparation and acid digestion techniques (Swart et al., 2019), choice of ^{17}O correction parameters (Daëron et al., 2016; Schauer et al., 2016), mineralogy and acid fractionation dependencies (Petersen et al., 2019), standardization of measurements (Bernasconi et al., 2021; Dennis et al., 2011), among others. For example, differences in calibration slopes among laboratories are partly due to the choice of ^{17}O correction parameters (International Union of Pure and Applied Chemistry [IUPAC]) parameters versus Gonfiantini parameters (Daëron et al., 2016; Gonfiantini et al., 1995; Schauer et al., 2016) adopted in the data processing. Thus, the use of IUPAC parameters is recommended since it allows convergence of most datasets to statistically similar calibration slopes within reasonable analytical uncertainties (Petersen et al., 2019). These parameter sets relate to the differences in the choice of the slope of the triple oxygen isotope line (λ) that describes the fractionation of ^{17}O relative to ^{18}O, and the absolute $^{13}C/^{12}C$ and $^{17}O/^{16}O$, $^{18}O/^{16}O$ ratios of VPDB and VSMOW, respectively (see Brand et al., 2010; Daëron et al., 2016 for details).

Given the recent progress in the development of the clumped isotope proxy and community-wise consensus on acquiring Δ_{47} data through carbonate based standardization (Bernasconi et al., 2021) and IUPAC parameters (Petersen et al., 2019), we revisit the Δ_{47}-T relationship published for otoliths (Ghosh et al., 2007) and further assess its applicability to select samples from a Miocene habitat. It must be noted that, the Ghosh et al. (2007) otolith calibration was derived based on Δ_{47} data acquired through the conventional heated gas anchors and Gonfiantini parameter sets. In addition, despite the potential for otolith clumped isotope composition as a useful paleo-climate archive, we are aware of a few studies assessing its reliability. For example, carbonate clumped-isotope thermometry was used to detect and reconstruct prehistoric processing methods in skeletal aragonitic molluscs (shells) and fish (otoliths) (Müller et al., 2017). In this paper, we reanalyzed some of the otoliths reported by Ghosh et al. (2007) and present new otolith analyses from the Natural History Museum of Los Angeles County (LACM), as part the recalibration exercise. The revised equation, calibrated in the absolute reference frame (Dennis et al., 2011) is validated by applying it to modern fish otoliths of *Lutjanus lutjanus* from the Bay of Bengal.

In addition, we apply our new relationship to lower Miocene (Burdigalian; ~17 Ma) otoliths of "genus Ambassidarum" sp. and "genus Gobiidarum" sp. from the Pozhikkara cliff section of the Quilon Formation, southwest India. The age interval (~17 to 15 Ma) corresponds to a global warming event, that is, Middle Miocene Climate

Table 1
Average Values of Δ_{47} of Otolith Aragonite Based on Three Replicates With Growth Temperature and Locations Samples Examined Corresponding to Figure 1

Sample description	Growth temperature (°C)	Latitude	Longitude	Depth (m)	Δ_{47} CDES	Δ_{47} error 1σ
Patagonotothen ramsayi	5.6 ± 2	54°39′S	57°9′W	124	0.740	0.027
Lutjanus malabaricus	25 ± 3	13°45′N	100°30′E	100	0.673	0.007
Coelorinchus sp. *Coelorhynchus*	9.7	55°12′N	09°55′W	50	0.722	0.013
Lutjanus synagris	27 ± 10	9°50′N	279°55′E	25	0.653	0.015
Reinhardtius hippoglossoides	3.4	57°21′N	180°42′E	250	0.722	0.004
Gadus morhua	7.5	56°30′N	2°30′E	50	0.725	0.008
Pogonias cromis	23 ± 5	23°54′S	314°57′E	30	0.686	0.014

Note. The uncertainties reported for growth temperatures are the temperature range of individual fish habitats from the location of sample collection. Please note that *Coelorinchus* sp., *Coelorhynchus*, *Reinhardtius hippoglossoides*, and *Gadus morhua* have no uncertainties reported due to narrow temperature habitat.

Optimum (MMCO; Zachos et al., 2001). During MMCO, the global annual surface temperature was on average about ∼3°C–4°C higher compared to present-day. Interestingly, climate models predict MMCO-like temperature conditions for the 22nd century given the current CO_2 emission rates (You, 2010; You et al., 2009). MMCO has been widely accepted as a possible analog of climate change in the future (Lee et al., 2021; You, 2010). Thus, it becomes crucial to understand the deep-time (Miocene) coastal water conditions to predict the future coastal water dynamics in the southwest of India. Herein, we show how new otolith-based temperature and δ^{18}O-water estimates can inform our understanding of coastal conditions, possibly in a region of upwelling during MMCO.

2. Analytical Methods

2.1. Otoliths Collection

2.1.1. Modern Otoliths

Otolith samples used for the calibration were collected from the John E. Fitch Otolith Collection housed in the Department of Ichthyology, LACM, USA. The selected specimens span seven different geographic locations and range in temperature from 3°C to 25°C (Table 1 and Figure 1). Samples from the LACM collection with their catalog number and their respective sampling locations are *Patagonotothen ramsayi* (11070_003, 54°39′S, 57°9′W), *Lutjanus malabaricus* (26509, 13°45′N, 100°30′E; Thailand, Bangkok), *Coelorinchus caelorhincus* (58251_001, 55°12′N, 09°55′W; Ireland, West of Donegal), *Lutjanus synagris* (58825_001, 9°50′N, 279°55′E; Panama), *Reinhardtius hippoglossoides* (58834_001, 57°21′N, 180°42′E; Bearing Sea), *Gadus morhua* (58835_001, 56°30′N, 2°30′E; North Sea), and *Pogonias cromis* (58836_1, 23°54′S, 314°57′E; Brazil, Santos). The fish habitats were retrieved from http://www.fishbase.org/home.htm (Froese & Pauly, 2021) for the individual fish species. We established average growth temperatures with a precision of ±2°C based on the latitude, longitude, and depth of the fish habitat using data from https://www.nodc.noaa.gov. The formation temperature of the carbonate in the fish otoliths was inferred to be the mean temperature of the habitat, averaged over the specimens' estimated lifetimes.

Additionally, five specimens of *L. lutjanus* otoliths were collected at Chennai, India from a commercial fishing catch from Bay of Bengal water in October 2011 with a typical fish weight ∼50–70 g. *L. lutjanus* species are "cold-blooded" (i.e., they cannot regulate their body temperature), schooling species that live around coral reefs and coastal areas in tropical marine waters of the Indo-West Pacific. The general habitat of these fishes is bathydemersal marine with a depth range of 0–96 m.

2.1.2. Fossil Otoliths

Fossil otolith samples belonging to "genus Ambassidarum" sp. and "genus Gobiidarum" sp. were recovered from the carbonaceous clay unit of Quilon Formation exposed at the Pozhikkara cliff section along the Kerala coast, southwest India (Figure 2). Based on previous studies, the depositional settings of the recovered otoliths were ascribed to be an open marine shelf with local coral reef occurrences in settings shallower than 20 m proximal to the coast (Narayanan et al., 2007; Raha et al., 1983). The age of the Quilon Formation is assigned as lower
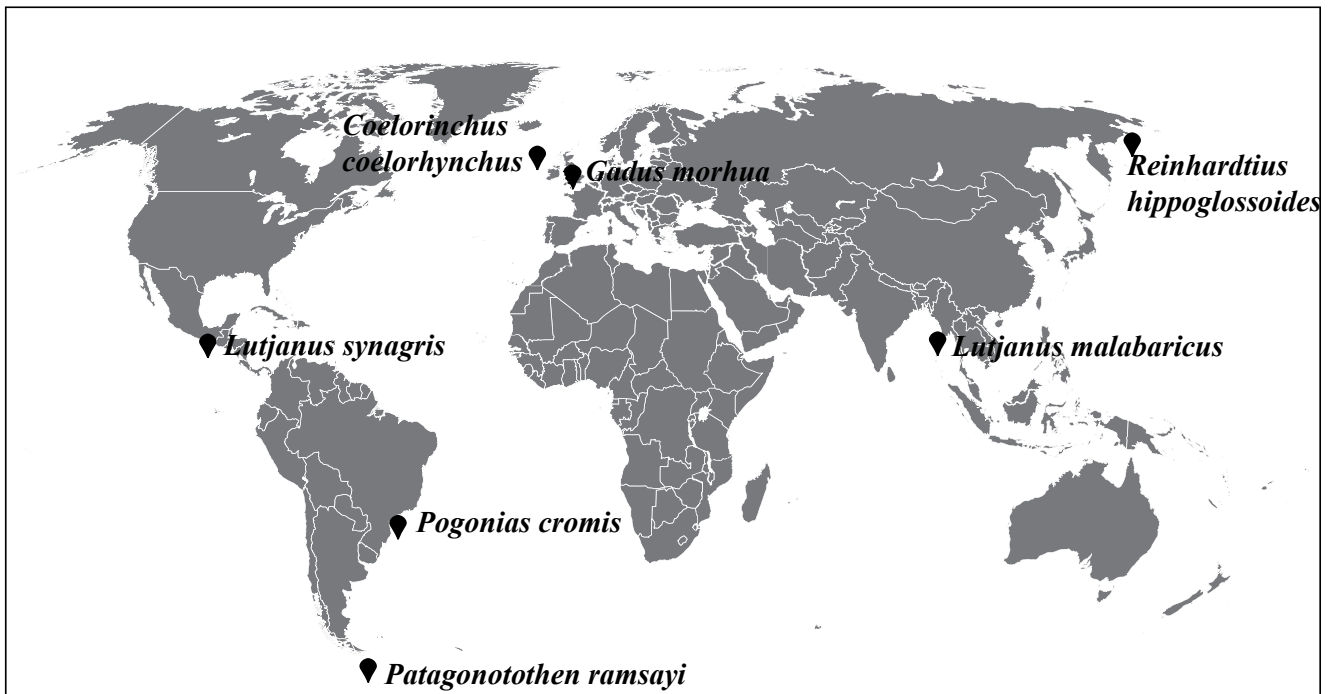
Figure 1. Locations of samples examined in this study, with the name of the fish species corresponding to the entries in Table 1.

Miocene (Burdigalian) based on the foraminiferal biostratigraphy (Jacob & Sastri, 1952; Raju, 1978; Rasheed & Ramachandran, 1978). This lower Miocene (Burdigalian) age also corresponds to the global warming event MMCO (~17–15 Ma). Details on the stratigraphy and age of the Quilon Formation are provided as Text S1 in Supporting Information S1.
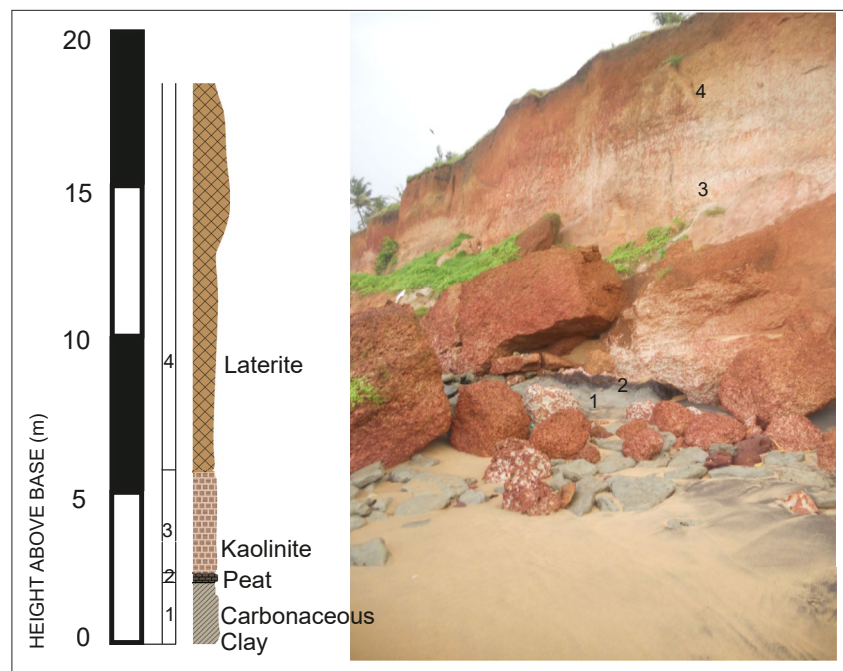
Figure 2. Geographic locations of Pozikkara cliff section, Quilon Formation, southwest India and its lithostratigraphy of the location. Miocene otoliths "genus Ambassidarum" and "genus Gobiidarum" were sampled from the carbonaceous clay layer of the section.

Geographically, modern-day Ambassid fishes (family Ambassidae) are widely distributed throughout the shallow waters of the Indo-Pacific region (i.e., South Africa, India, New Guinea, and Australia) (Martin & Heemstra, 2015) while Gobiids (Family: Gobiidae) are essentially marine and brackish water, bottom dwellers sustaining tropical and sub-tropical shallow waters.

The lower Miocene (Burdigalian) fish otolith specimens for paleo-temperature reconstruction were recovered following the procedure as described in Kapur et al. (2019), but, without the utilization of chemicals. Preservation of otoliths was assessed using SEM and cathodoluminescence imaging of thin sections and XRD analysis of powder (Text S2 and S3 in Supporting Information S1). The results suggest that the analyzed otoliths have a composition of ∼ >85% aragonite, and the trace element geochemistry is consistent with minimum diagenetic alteration. However, the fact that otoliths are not 100% aragonite suggests some alteration.

2.2. Carbonate Clumped Isotope Thermometry

Carbonate clumped isotope paleo-thermometry is based upon the principle that the formation temperature of carbonates is proportional to the relative abundance of $^{13}C^{18}O^{16}O_2$ in carbonate ion groups determined through the measurement of $^{13}C^{18}O^{16}O$ in CO_2 generated through acid digestion. The abundance of these multiply substituted isotopologues in carbonate minerals is governed by thermodynamic parameters (Hill et al., 2014, 2020; Pramanik et al., 2020; Schauble et al., 2006) that depend on the rotational and vibrational frequencies of the relevant bonds. Precise measurements that determine the abundance of isotopologues containing multiple heavy isotopes ($^{13}C^{18}O$) in the CO_2 provides information about the temperature during the formation of the carbonate. The carbonate clumped isotope abundance (Δ_{47}) in permil (‰) is calculated as follows:

$$\Delta_{47} = \left[\frac{R^{47}}{2R^{13}R^{18} + 2R^{17}R^{18} + R^{13}\left(R^{17}\right)^2} - \frac{R^{46}}{2R^{18} + 2R^{13}R^{17} + \left(R^{17}\right)^2} - \frac{R^{45}}{R^{13} + 2R^{17}} + 1 \right] \quad (1)$$

Sample R^{47} ratios are normalised to a reference gas whose composition has achieved a stochastic distribution. The ratios of R^{45} and R^{46} are used to calculate the $^{13}C/^{12}C$, $^{18}O/^{16}O$, and $^{17}O/^{16}O$ ratios (R^{13}, R^{18}, and R^{17}, respectively) for the sample. In our data reduction, we use the IUPAC parameter set ($\lambda = 0.528$, $R^{13}_{VPDB} = 0.01118$, $R^{18}_{VSMOW} = 0.00200520$, and $R^{17}_{VSMOW} = 0.00038475$) as recommended by Brand et al. (2010).

2.3. Sample Treatment for Carbonate Clumped Isotope Analysis

The modern fish otoliths of *L. lutjanus* from the Bay of Bengal and the lower Miocene (Burdigalian) fossil otoliths specimens belonging to "genus Ambassidarum" sp. and "genus Gobiidarum" sp. used for proxy validation and paleo-environment reconstruction were analyzed in the OASIS Stable Isotope Lab, Centre for Earth Sciences, Indian Institute of Science (IISc), Bangalore, following the "breakseal" method described in Fosu et al. (2019). All samples were cleaned with 30% H_2O_2 for 12 hr to remove any organic material. The samples were subsequently weighed, finely crushed, and stored in glass vials. An aliquot weighing ∼5–8 mg was digested individually by reacting with anhydrous 105% phosphoric acid (H_3PO_4) at 25°C; for several hours (>16 hr). The produced CO_2 was extracted cryogenically in a vacuum line apparatus using liquid nitrogen (at ∼−196°C) and an ethanol + liquid nitrogen "slush" (held at ∼−90°C). In this way, the CO_2 was transferred through a series of U-traps avoiding potential re-equilibration with H_2O. The CO_2 gas (devoid of H_2O and other trace gases) was further purified to remove organic and other potential contaminants (hydrocarbons and halocarbons) by use of a gas chromatograph (custom-made Porapaq-Q column, 2 m length, 1/8″ diameter, 80–100 mesh) held at −10°C. Samples gas was transferred through the Porapaq trap using ultra-high purity He streams at 10 mL/min. CO_2 yields were monitored with a capacitance manometer before and after cleaning to ensure complete transfer; samples with low yield were discarded. The purified CO_2 was analyzed in dual-inlet mode on a Thermo Fisher Scientific MAT 253 mass spectrometer within a few hours after cleaning.

The MAT 253 Isotope Ratio Mass Spectrometer (IRMS) was configured to simultaneously analyze masses 44–49 of CO_2. Masses 47–49 were measured with 10^{12} Ω resistors. Masses 48 and 49 were monitored to ensure that there were no isobaric interferences due to the presence of contaminants (Huntington et al., 2009), given that

these interferences can lead to spurious Δ_{47} measurements. Each analysis involved 60 measurement cycles of the sample CO_2 and reference CO_2 (six acquisition lines with 10 cycles each, with a signal integration time of 8 s). The compression in the dual inlet bellows was sufficient to maintain the CO_2 mass-44 ion beam intensity at a voltage of 10–12 V for the start of each acquisition. Sample analyses were covered in two different sessions. The analysis for modern fish otoliths of *L. lutjanus* from the Bay of Bengal was carried out in June-August 2013. The working gas (a high purity 99.999% CO_2 from Linde AG, Munich, Germany) used in this session has a composition of $\delta^{13}C$: $-4‰$ VPDB and $\delta^{18}O$: 25.19‰ VSMOW. Otoliths specimens belonging to "genus Ambassidarum" sp. and "genus Gobiidarum" sp., from the Quilon Formation, were analyzed in February 2019. The composition of the working gas during this period was $-3.92‰$ and 25.58‰ for $\delta^{13}C$ and $\delta^{18}O$, respectively.

Modern otoliths from LACM used for the revised calibration experiment were analyzed in the Tripati Stable Isotope Lab at the University of California Los Angeles (UCLA), using methods described in Defliese and Tripati (2020). All otolith samples were finely crushed and stored in glass vials. The NuCarb automated carbonate device, interfaced with the Nu Instruments Perspective IRMS, allows small amounts of carbonate samples (15–150 µg) to be reacted in separate reaction vials maintained at 70°C. The pre-weighed samples along with carbonate standards, including ETH 1–4 (Bernasconi et al., 2018), as well as several in-house standards, were loaded into individual vials and reacted sequentially by controlled injection of ~1 ml of phosphoric acid. The evolved CO_2 was purified using a Porapak trap and transferred cryogenically through a series of cold finger apparatus whose temperature is regulated by varying the amount of liquid nitrogen. The cleaned gas was ultimately transferred via micro inlet followed by isotopic measurement on the high resolution, high sensitivity Nu Perspective IRMS. Crucial steps such as vial positioning, the vial pump out, delivery of acid, CO_2 collection, sample clean-up, and transfer via the micro-volume, matching of reference, and sample intensities before data acquisition were all automated.

The Nu Instruments Perspective mass spectrometer at UCLA is a relatively new design. The Perspective has a Nier-type ion source and magnetic sector; however, it features a pair of quadratic lenses after the magnetic sector, and cups 47, 48, and 49 are shielded by small electrostatic sector analyzer that can be tuned to screen out secondary background ions. Analyses were performed in micro-volume mode, with balanced sample and reference gas volumes that allow the gas to deplete at precisely matched rates, thereby increasing the efficacy of gas usage. Each cycle lasts around 60 s, and measurements range from 70 to 30 nA for the mass 44 signal. The working gas used was Oztech CO_2 (Safford, AZ, USA) that has a $\delta^{13}C$ value of $-3.6‰$ (VPDB) and $\delta^{18}O$ value of 25.0‰ (VSMOW).

2.3.1. Standardization

The evaluation of Δ_{47} data in both IISc and UCLA laboratories follow a near-identical approach. Differences arise from the full carbonate-based standardization scheme used in UCLA whereas a combination of equilibrated gases and carbonate standards were used in the IISc lab. Δ_{47} values of carbonate standards common to both labs are however comparable and are within the analytical uncertainties of measurements in the respective laboratories. For example, Carrara marble from UCLA (CM Tile) yielded a mean value of 0.380 ± 0.028 (1σ, $n = 20$), whereas, Carrara marble standard from IISc (MARJ1) yielded a mean value of 0.393 ± 0.025 (1σ, $n = 14$).

Briefly, Δ_{47} results at IISc were standardized using a set of equilibrated CO_2 gases of varying bulk isotopic composition in combination with several carbonate standards (Carrara-1, OMC, IAEA-603, NBS-19, and NBS-18). The CO_2 gases were equilibrated at 25°C by exchange with water for a minimum of 72 hr and at 1,000°C by heating in an oven (in flame-sealed quartz tubes) for 2 hr. All equilibrated gases were subject to the same cleaning and handling procedure as carbonate samples/standards, as discussed above, except that they were not reacted with phosphoric acid. The analytical data were evaluated using the Easotope software (John & Bowen, 2016).

At UCLA, a carbonate based standardization method (Bernasconi et al., 2018, 2021; Defliese & Tripati, 2020; Upadhyay et al., 2021) involving carbonate standards (ETH 1–4) of varying bulk isotopic and Δ_{47} composition was used. The performance of the mass spectrometer and the consistency of the carbonate-based standardization were monitored using additional standards such as IAEA-C1, IAEA-C2 and Merck and in-house carbonate standards such as Carrara marble, Veinstrom, CM Tile, and Caramel Chalk. The carbonate based normalization has the benefit of avoiding the time intensive preparation of equilibrated gases, and ensuring identical treatment of both standards and samples. However, this requires analyzing multiple standards during the run (preferably

a 50:50 sample to standard ratio), reducing sample throughput. All the data were processed using the Easotope software (John & Bowen, 2016)

The external precision (calculated from replicate analyses of an in-house laboratory standard) was 0.05‰ for $\delta^{13}C$ and 0.1‰ for $\delta^{18}O$. The external precision of Δ_{47} measurements was typically 0.03‰, which is consistent with the shot-noise limits for ion-beam intensities and the analytical duration (≥ 1 hr) consisting of several repeat analysis of sample CO_2. Furthermore, R^{48} and R^{49} values were routinely monitored for all sample gases as a quality check.

2.4. Reconstruction $\delta^{18}O$ and $\delta^{13}C$ of the Environmental Water

The environmental water composition of present day Bay of Bengal was determined using the relationship between temperature and the $^{18}O/^{16}O$ fractionation factor in marine habitat (1,000 ln α = 18.56 (10^3 TK^{-1}) – 32.54) by Thorrold et al. (1997). Since previous studies have indicated the depositional settings to be shallow marine proximal to the coast (Narayanan et al., 2007; Raha et al., 1983), the paleo-environmental water composition was determined assuming a brackish habitat (1,000 ln α = 18.39 (10^3 TK^{-1}) – 34.56) by Willmes et al. (2019). The effect of the choice of fractionation factor on the final reconstructed $\delta^{18}O$-water is discussed in Text S4 in Supporting Information S1. Carbon isotope ratios of the samples were also used to estimate the $\delta^{13}C$ composition of paleo-water using a mass balance approach (Kalish, 1991a). First, the percentage of metabolically derived carbon in the modern otoliths was calculated using the $\delta^{13}C$ values, $\delta^{13}C$ of seawater, and carbon reservoirs in the form of metabolic by-products (Text S5 in Supporting Information S1). Following Kalish (1991b), the proportional contribution of metabolic carbon in the body fluid was estimated, from which the paleo-seawater $\delta^{13}C$ was subsequently derived.

3. Results

3.1. Revised Otolith Calibration

Normalization schemes for Δ_{47} values can affect data interpretation, thus, we herein consider two prominent scales, the traditional Carbon Dioxide Equilibrium Scale (CDES) and the recently introduced Intercarb-Carbon Dioxide Equilibrium Scale (I-CDES).

First, we compare the mean Δ_{47} value determined for each otolith sample against independent constraints on growth temperature as shown in Figure 3. The equation obtained for otoliths on the CDES, anchored to the ETH 1–4 standards (Bernasconi et al., 2018), is as follows:

$$\Delta_{47\,CDES} = 0.0364 \pm 0.005 \times \frac{\left(10^6\right)}{T^2} + 0.2619 \pm 0.0657 \left(R^2 = 0.9, p - \text{value} < 0.001\right) \tag{2}$$

If we use the newly determined nominal Δ_{47} values for the ETH standards, in addition to IAEA-C1 and IAEA-C2 and the equation obtained for otoliths on the I-CDES, is as follows:

$$\Delta_{47\,I\text{-}CDES} = 0.0353 \pm 0.005 \times \frac{\left(10^6\right)}{T^2} + 0.2781 \pm 0.0682 \left(R^2 = 0.89, p - \text{value} < 0.001\right) \tag{3}$$

where Δ_{47} is in ‰, T (temperature) is in K, and the two-tailed p-values are calculated using a t-test. Even if the carbonate standards anchored to the otolith data set are limited to ETH 1–4 (as in Equation 2), the Δ_{47}-T calibration equation in I-CDES is indistinguishable from Equation 3.

A comparison of these results to other published calibrations that were derived using the same IUPAC parameter set and data normalization (Bernasconi et al., 2018; Defliese & Tripati, 2020; Jautzy et al., 2020; Petersen et al., 2019) is illustrated in Figure 3. These studies employed either a fully carbonate-based standardization as adopted in this study (Bernasconi et al., 2018; Jautzy et al., 2020) or equilibrated gases or a combination of equilibrated gases and carbonate standards (Defliese & Tripati, 2020; Petersen et al., 2019).
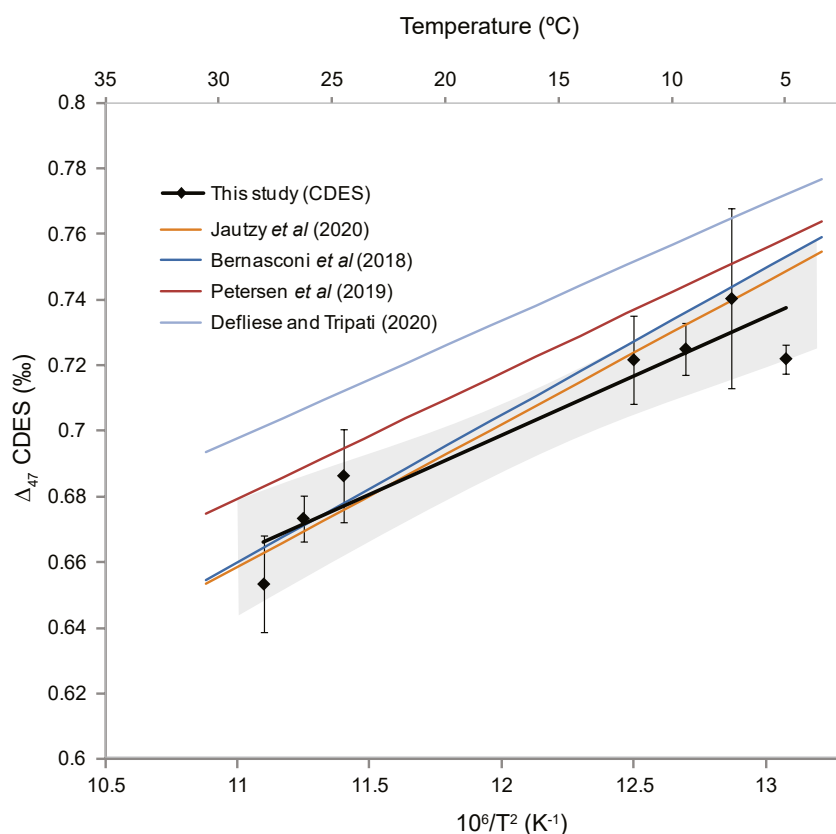
Figure 3. Relationship between estimated environmental temperatures at which sampled fishes lived and Δ_{47} values of CO_2 produced by phosphoric acid digestion of fish otoliths (plotted as filled diamond). Two-tailed p-values are calculated using a t-test and the error bars for the offset Δ_{47} values indicate the 1σ S.E. Other Δ_{47}-temperature equations derived using the IUPAC set of isotopic parameters are shown for comparison. Bernasconi et al. (2018) and Jautzy et al. (2020) at a carbonate reaction temperature of 70°C. Petersen et al. (2019) and Defliese et al. (2015) calibration was replicated and recalculated in Defliese and Tripati (2020), the carbonate reaction temperature was 25°C. The linear regression is calculated here using SigmaPlot (Systat Software, San Jose, CA).

3.2. Modern Otoliths

The results of five modern Bigeye snapper (*L. lutjanus*) otoliths from the Bay of Bengal are plotted in Figure 4. The average $\delta^{18}O$ and $\delta^{13}C$ values of five individual samples analyzed in this study are -1.94 ± 0.3‰ and -4.1 ± 0.29‰, respectively. The reconstructed body temperature based on clumped isotope analysis suggests a range of 18.4°C–28.4°C and a mean value of 22.3°C $\pm$ 4.2°C in comparison to 25°C–28.5°C in the mixed layer of Bay of Bengal observed in the modern day (Anilkumar et al., 2006).

3.3. Reconstruction of Lower Miocene (Burdigalian) Water Temperature ("genus Ambassidarum" sp. and. "genus Gobiidarum" sp.)

The results of five Miocene otoliths from the Quilon Formation are shown in Figure 4. The bulk otolith samples of four specimens belonging to "genus Ambassidarum" sp. yielded mean $\delta^{18}O$ and $\delta^{13}C$ values of -3.8 ± 0.5‰ and -3.4 ± 0.5‰, respectively. The corresponding Δ_{47} values range from 0.702 to 0.709‰ (mean 0.705 $\pm$ 0.003‰). The estimated range of Δ_{47} based temperatures in the "genus Ambassidarum" sp. is 12.1°C–14.3°C (mean 13.5°C $\pm$ 1°C), while Δ_{47}-T obtained for "genus Gobiidarum" sp. is 10.2°C. The reconstructed environmental water composition for "genus Ambassidarum" sp. is in the range of -3.5 to -2.6‰ (mean -2.9 ± 0.4‰). For "genus Gobiidarum" sp. the $\delta^{18}O$ and $\delta^{13}C$ values are -4.5‰ and -4.86‰, respectively, while the Δ_{47} composition is 0.715‰. The environmental water composition reconstructed from "genus Gobiidarum" sp. is -4.4‰.
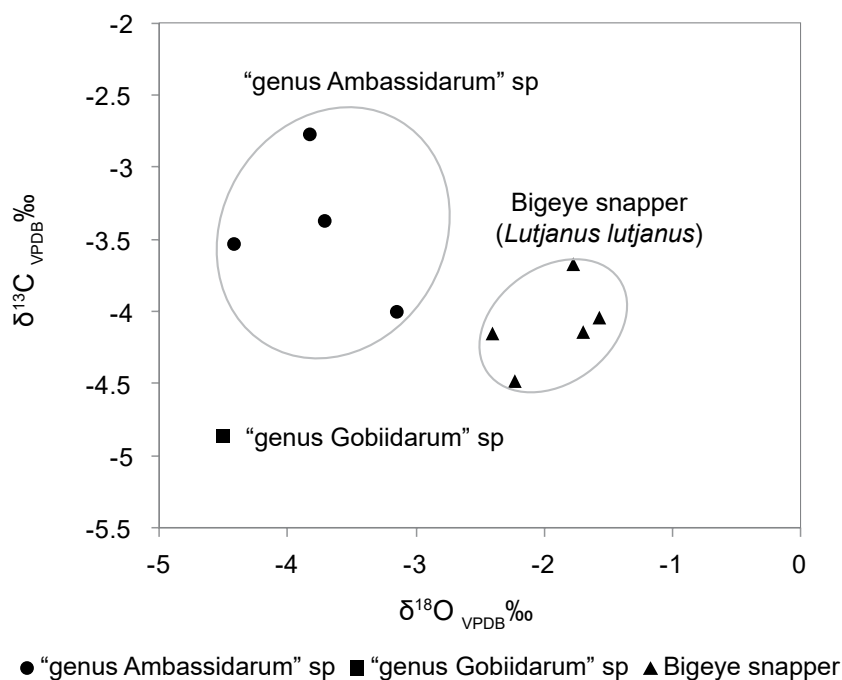
Figure 4. Cross-comparison of $\delta^{13}C$ and $\delta^{18}O$ from fish otoliths. The otoliths were obtained from modern species from the Bay of Bengal (*Lutjanus lutjanus*, Triangle, $n = 5$), Miocene "genus Ambassidarum" collected from the Quilon Formation (Circles, $n = 4$), and Miocene "genus Gobiidarum" collected from the Quilon Formation (Square, $n = 1$).

4. Discussion

4.1. The Effect of ^{17}O Correction and Data Standardization on Δ_{47}-T Calibration

The revised Δ_{47}-T calibration equation for otolith using the IUPAC parameters yields a slope and intercept of 0.0364 ± 0.005 and 0.2642 ± 0.0657, respectively. In contrast, using the Gonfiantini parameters the calibration yield a calibration slope and intercept of 0.0335 ± 0.005 and 0.2956 ± 0.0664, respectively (Text S6 in Supporting Information S1). These slopes and intercepts obtained using the different isotopic parameter sets are statistically indistinguishable and the maximum difference in reconstructed temperatures at a given calibration point is 0.7°C which is within the analytical uncertainty of our measurements. This suggests that the use of carbonate-based standardization minimizes potential differences between the slopes and intercepts in comparison to the exclusive use of equilibrated gases. In effect, the dependence of the calibration on the choice of ^{17}O correction parameters is minimized following consistent normalization of Δ_{47} data with carbonate standards.

Despite the agreement in the different slopes and intercepts (using IUPAC vs. Gonfiantini parameters) for the otolith calibration, minor differences remain when compared to other Δ_{47}-T calibrations that also adopt a full carbonate-based standardization or intersperse carbonates with equilibrated gases such as those from Bernasconi et al. (2018), Jautzy et al. (2020), Defliese and Tripati (2020), and Petersen et al. (2019). Besides the differences in mineralogy (calcite, aragonite, dolomite, or a composite) and sample types (inorganic, biogenic or a mix), it is clear from Figure 3 that calibration slopes are probably sensitive to methodological differences amongst laboratories. For the Δ_{47}-T otoliths calibration, the differences in slopes for both CDES and I-CDES are statistically significant ($P = 0.046$ see Text S7 in Supporting Information S1 for details). The slope of the Defliese and Tripati (2020) calibration is identical to the slope of the otolith data set (this study; both data sets generated in the same laboratory) which is not the case for the other published calibrations (Figure 3). The recent Intercarb standardization exercise (Bernasconi et al., 2021) and uncertainty propagation methods (Daëron, 2021) aim to resolve these inter-laboratory differences.

In addition to the substantial errors in reconstructed temperature introduced by analytical uncertainties and other uncertainties related to the slopes and intercepts of Δ_{47}-T calibrations, recent studies suggest that the direct measurement of triple oxygen isotope compositions ($\Delta^{17}O$) of reference materials may improve the accuracy

Table 2
Data for Bigeye Snapper (Lutjanus lutjanus) From the Bay of Bengal

Bigeye snapper (*L. lutjanus*)					
	Δ_{47} CDES scale	Reconstructed formation temperature (°C)	$\delta^{18}O$ carbonate rel. to VSMOW	α	$\delta^{18}O$ water rel. to VSMOW
OL 1	0.662	28.5	28.61	1.029	−0.78
OL 2	0.685	20.1	29.16	1.031	−2
OL 3	0.686	19.8	29.08	1.031	−2.15
OL 6	0.672	24.8	28.43	1.030	−1.72
OL 7	0.690	18.4	29.29	1.032	−2.24

Note. $\delta^{18}O$ water was calculated based on the temperature-dependent fractionation equation from Thorrold et al. (1997). Oxygen isotope signals of Bay of Bengal surface waters during the winter months of November to February is <−1‰ (Achyuthan et al., 2013).

and precision of Δ_{47} determinations (Saenger et al., 2021). Traditionally, laboratories assume the $\Delta^{17}O$ value of the carbonates (or CO_2 analyte) to be zero (i.e., $\Delta^{17}O = 0$). Such an assumption has the potential to yield small inaccuracies in Δ_{47} reconstructed values, depending on the composition of the mass spectrometer working gas and data normalization procedures, that can potentially be up to 0.6°C–5.8°C (Saenger et al., 2021). While the choice of ^{17}O correction parameters yields negligible differences in the slopes and intercepts of the otolith Δ_{47}-T calibrations (anchored to ETH standards), the use of the accurate $\Delta^{17}O$ values of these and other commercial standards (Fosu et al., 2020; Saenger et al., 2021; Wostbrock et al., 2020) may improve the agreement between inter-laboratory calibrations and the overall accuracy of Δ_{47} measurements.

4.2. Bigeye Snapper (*L. lutjanus*)

The reconstructed temperature of 22.3°C (this study) is within ±2°C of the previously measured sea surface temperature (SST) over the coastal Bay of Bengal (Anilkumar et al., 2006). The $\delta^{18}O$ of water reconstructed from otoliths belonging to *L. lutjanus* is −1.7 (±0.5‰) (Table 2) which is identical to previously reported depleted oxygen isotope signals (i.e., $\delta^{18}O$ is <−1‰) for the Bay of Bengal surface waters during the winter months of November to February (Achyuthan et al., 2013).

4.3. Miocene Reconstruction

The lower Miocene (Burdigalian) strata that were sampled fall within a unique geologic time referred to as the "Middle Miocene Climatic Optimum (MMCO)" when the global annual surface temperatures were on average about ∼3°C–6°C higher compared to present-day and pCO_2 levels were similar to modern levels (Böhme, 2003; Tripati et al., 2009). In the present study, the estimated range of Δ_{47} based temperatures in the "genus Ambassidarum" sp. is 12.1°C–14.3°C (mean: 13.5°C ± 1°C), while Δ_{47} temperature obtained for "genus Gobiidarum" sp. is 10.2°C (Table 3). These reconstructed temperatures are significantly lower than those inferred from pollen, Mg/Ca and fossil records. Reuter et al. (2013) in their report on the Early/Middle Miocene (∼17–15 Ma) pollen assemblages from the siliciclastic Ambalapuzha Formation at the coastal cliffs of Varkala in southwest Kerala, India, suggested a mean annual air temperature of 22.2°C–26.6°C based on the coexistence approach. However, Mg/Ca-SST based temperature estimates from mixed layers in the Eastern Arabian Sea (EAS) off the coast of western India suggest a temperature of ∼27.7°C between ∼16 and 15 Ma (Yang et al., 2020).

Table 3
Data for Otoliths Belonging to "Genus Ambassidarum" sp., and "Genus Gobiidarum" sp. Recovered From the Quilon Formation

	Δ_{47} CDES scale	Reconstructed formation temperature (°C)	$\delta^{18}O$ carbonate rel. to VSMOW	α	$\delta^{18}O$ water rel. to VSMOW
"genus Ambassidarum" sp.					
PK_1	0.709	12.1	27.6	1.030	−2.6
PK_2	0.702	14.4	27.0	1.030	−2.7
PK_3	0.704	13.7	26.3	1.030	−3.5
PK_7	0.703	14.1	26.9	1.030	−2.9
"genus Gobiidarum" sp.					
PK_4	0.715	10.2	26.2	1.031	−4.4

Note. $\delta^{18}O$ water was calculated based on temperature-dependent fractionation equation from Thorrold et al. (1997).

Because other proxies point to the higher atmospheric and mixed layer temperatures, we interpret the cooler temperatures inferred from our analysis of otoliths to reflect formation in an upwelling environment. Fewer studies (Faul et al., 2000; Peeters et al., 2002) on modern and fossil foraminifera have shown that organisms that calcify in an upwelling environment yield higher $\delta^{18}O$ values and lower $\delta^{13}C$ values. Faul et al. (2000) used the relationship between modern surface hydrography and core-top planktonic foraminiferal abundances and their isotopic composition to interpret upwelling and productivity changes in the eastern equatorial Pacific over the last 20,000 years. Peeters et al. (2002) based on the oxygen isotope composition of the foraminifera shells and vertical shell concentration profiles suggest that the depth habitat for planktonic foraminifera species (*Globigerina bulloides* and *Globigerinoides ruber*) is shallower during upwelling. Further, the carbon isotope composition recorded in the above-mentioned foraminifera species decreases as a result of lower dissolved inorganic carbon ($\delta^{13}C_{DIC}$) values in upwelled waters. Our reconstructed $\delta^{13}C$ values of ambient seawater are between −1.5‰ and −0.2‰ compared to previously reported $\delta^{13}C_{DIC}$ 0.5‰–0.9‰ for Arabian Sea surface waters (Prasanna et al., 2016). There exists a relationship between otoliths $\delta^{13}C$ and reconstructed temperature (Text S8 in

Supporting Information S1). This value could indicate that in this region, the fish were at or near the coast with carbon input from either surface runoff or through the resurgence of cold bottom water with isotopically lighter carbon to the surface. The recorded changes in the isotopic values and temperatures (this study) may be attributed to localized upwelling considering that previous literature generally argues that upwelling causes higher $\delta^{18}O$ and lower $\delta^{13}C$ values, in response to mixing with upwelled deeper, colder waters. Recently, Bertucci et al. (2018) utilized stable isotopes on modern Whitemouth croaker otoliths to test for upwelling conditions. Their results suggest that otolith samples from the eastern coast of Brazil, grown under the direct influence of the Cabo Frio upwelling were characterized by their low water temperatures and higher $\delta^{18}O$-lower $\delta^{13}C$ values compared to Whitemouth croaker otoliths from the western coast of Brazil which grew under less upwelling influence. It is interesting to note that, several previous studies have also argued in favor of the prevalence of monsoonal upwelling in the Southern Arabian Sea during the Miocene (Gupta et al., 2015; Singh et al., 2011; Zhuang et al., 2017).

In the present study, the environmental water $\delta^{18}O$ composition calculated from the "genus Ambassidarum" sp. yielded a value between $-3.5‰$ and $-2.6‰$ (V-SMOW) (mean: $-2.9‰ \pm 0.4$) while of "genus Gobiidarum" sp. is $-4.4‰$. However, reported local $\delta^{18}O$ values for seawater varies between $\sim-0.82‰$ and $1.99‰$ during the middle Miocene (~16 to 11 Ma) interval (Yang et al., 2020). We consider here two possibilities: (a) cryptic diagenesis in the altered part of the otoliths that show ultrastructure and mineralogy preserved (see Wang et al., 2020), and (b) that the changes in the $\delta^{18}O$ values are due to kinetic effects impacting the $\delta^{18}O$ of fish otoliths independently of Δ_{47} (see Ghosh et al., 2006; Kimball et al., 2016; Thiagarajan et al., 2011).

An assessment of diagenetic effects on the samples (using cathodoluminescence imaging and XRD) suggest that the otoliths are composed of $\sim>85\%$ aragonite. The presence of secondary calcites may be due to the dissolution and reprecipitation of aragonite caused by the rapid influence of the hydrologic regime on the unstable otoliths aragonite under certain conditions (Weiner, 2010). The secondary calcite preferentially precipitated at ambient conditions because it is more stable than aragonite. They likely precipitated from an extraneous solution that enabled aragonite dissolution. Through this mechanism, the original composition of the otolith and isotopic signatures can be compromised. The dissolution and reprecipitation occurs on a nanoscale and affects the surface of single aragonite crystals. Therefore, a very small quantity of water is sufficient to trigger the reaction (Pingitore, 1976).

The latter scenario (kinetic effects) is also likely in the analyzed fish otoliths, causing changes in their $\delta^{18}O$ values. Resolving biases due to kinetic effects in (bio) mineralized carbonates would be enhanced by paired Δ_{47} and Δ_{48} in future investigations, enabling further constraints on the processes responsible for isotopic disequilibrium (Bajnai et al., 2020).

5. Conclusions

We present a new Δ_{47}-T calibration based on modern fish otolith. The revised calibration equation $\Delta_{47\,CDES} = 0.0364 \pm 0.005 \times \dfrac{\left(10^6\right)}{T^2} + 0.2619 \pm 0.0657 \left(R^2 = 0.9, p-\text{value} < 0.001\right)$, is unique for otoliths and is statistically different from the other Δ_{47}-T calibration curves. The calibration was used to estimate the body temperatures of Bigeye snapper (*L. lutjanus*). The reconstructed temperature of 22.3°C is within ±2°C of the SST measured over the coastal Bay of Bengal (Anilkumar et al., 2006). The $\delta^{18}O$ of water reconstructed from these otoliths is $-1.7‰$ (±0.5) which closely matches with the depleted oxygen isotope signals of Bay of Bengal surface waters during the winter months of November to February (Achyuthan et al., 2013), hence demonstrating the validity of the proposed Δ_{47}-T calibration.

In addition, we attempt to quantify lower Miocene (Burdigalian) coastal conditions in southwest India utilizing fossil otoliths. The revised Δ_{47}-T calibration, which was successfully tested in the case of modern *L. lutjanus* otoliths from the Bay of Bengal was applied to lower Miocene (Burdigalian) otoliths herein identified as belonging to "genus Ambassidarum" sp. and "genus Gobiidarum" sp. The clumped isotope-based temperature estimates (this study) of 12.1°C–14.3°C (mean: 13.5°C $\pm$ 1°C) for "genus Ambassidarum" sp., and 10.2°C for "genus Gobiidarum" sp. certainly provides constraints on coastal conditions, possibly in a region of upwelling during the MMCO, although we can not preclude diagenesis. The present investigation also opens future research avenues for assessing and predicting the coastal ecosystem in a warm climate. However, the readers should be cautious about the presence of kinetic effects influencing $\delta^{18}O$ or cryptic diagenesis with aragonite-aragonite

neomorphism. Use of micro-FTIR or Raman should be encouraged in future investigations to determine the degrees of structural ordering in relatively small areas (e.g., Sibony-Nevo et al., 2019) and also simultaneous measurement of Δ_{47} and Δ_{48} to decipher the kinetic effects in (bio) mineralized carbonates.

Conflict of Interest

The authors declare no conflicts of interest relevant to this study.

Data Availability Statement

Data is available at https://data.mendeley.com/datasets/skcz3ztg4f/4.

References

Achyuthan, H., Deshpande, R. D., Rao, M. S., Kumar, B., Nallathambi, T., Kumar, K. S., et al. (2013). Stable isotopes and salinity in the surface waters of the Bay of Bengal: Implications for water dynamics and palaeoclimate. *Marine Chemistry*, *149*, 51–62. https://doi.org/10.1016/j.marchem.2012.12.006

Anilkumar, N., Sarma, Y. V. B., Babu, K. N., Sudhakar, M., & Pandey, P. C. (2006). Post-tsunami oceanographic conditions in southern Arabian Sea and Bay of Bengal. *Current Science*, *90*, 421–427.

Bajnai, D., Guo, W., Spötl, C., Coplen, T. B., Methner, K., Löffler, N., et al. (2020). Dual clumped isotope thermometry resolves kinetic biases in carbonate formation temperatures. *Nature Communications*, *11*(1), 4005. https://doi.org/10.1038/s41467-020-17501-0

Bernasconi, S. M., Daëron, M., Bergmann, K. D., Bonifacie, M., Meckler, A. N., Affek, H. P., et al. (2021). InterCarb: A community effort to improve interlaboratory standardization of the carbonate clumped isotope thermometer using carbonate standards. *Geochemistry, Geophysics, Geosystems*, *22*(5), e2020GC009588. https://doi.org/10.1029/2020GC009588

Bernasconi, S. M., Müller, I. A., Bergmann, K. D., Breitenbach, S. F. M., Fernandez, A., Hodell, D. A., et al. (2018). Reducing uncertainties in carbonate clumped isotope analysis through consistent carbonate-based standardization. *Geochemistry, Geophysics, Geosystems*, *19*(9), 2895–2914. https://doi.org/10.1029/2017GC007385

Bertucci, T., Aguilera, O., Vasconcelos, C., Nascimento, G., Marques, G., Macario, K., et al. (2018). Late Holocene palaeotemperatures and palaeoenvironments in the Southeastern Brazilian coast inferred from otolith geochemistry. *Palaeogeography, Palaeoclimatology, Palaeoecology*, *503*, 40–50. https://doi.org/10.1016/j.palaeo.2018.04.030

Böhme, M. (2003). The Miocene Climatic Optimum: Evidence from ectothermic vertebrates of Central Europe. *Palaeogeography, Palaeoclimatology, Palaeoecology*, *195*(3–4), 389–401. https://doi.org/10.1016/S0031-0182(03)00367-5

Brand, W., Assonov, S., & Coplen, T. (2010). Correction for the 17O interference in δ13C measurements when analyzing CO_2 with stable isotope mass spectrometry (IUPAC Technical Report). *Pure and Applied Chemistry*, *82*, 1719–1733. https://doi.org/10.1351/PAC-REP-09-01-05

Campana, S. E., & Neilson, J. D. (1985). Microstructure of fish otoliths. *Canadian Journal of Fisheries and Aquatic Sciences*, *42*(5), 1014–1032. https://doi.org/10.1139/f85-127

Daëron, M. (2021). Full propagation of analytical uncertainties in Δ_{47} measurements. *Geochemistry, Geophysics, Geosystems*, *22*(5), e2020GC009592. https://doi.org/10.1029/2020GC009592

Daëron, M., Blamart, D., Peral, M., & Affek, H. P. (2016). Absolute isotopic abundance ratios and the accuracy of Δ_{47} measurements. *Chemical Geology*, *442*, 83–96. https://doi.org/10.1016/j.chemgeo.2016.08.014

Defliese, W. F., Hren, M. T., & Lohmann, K. C. (2015). Compositional and temperature effects of phosphoric acid fractionation on Δ47 analysis and implications for discrepant calibrations. *Chemical Geology*, *396*, 51–60. https://doi.org/10.1016/j.chemgeo.2014.12.018

Defliese, W. F., & Tripati, A. (2020). Analytical effects on clumped isotope thermometry: Comparison of a common sample set analyzed using multiple instruments, types of standards, and standardization windows. *Rapid Communications in Mass Spectrometry*, *34*(8), e8666. https://doi.org/10.1002/rcm.8666

Dennis, K. J., Affek, H. P., Passey, B. H., Schrag, D. P., & Eiler, J. M. (2011). Defining an absolute reference frame for 'clumped' isotope studies of CO_2. *Geochimica et Cosmochimica Acta*, *75*(22), 7117–7131. https://doi.org/10.1016/j.gca.2011.09.025

Eiler, J. M. (2011). Paleoclimate reconstruction using carbonate clumped isotope thermometry. *Quaternary Science Reviews*, *30*(25), 3575–3588. https://doi.org/10.1016/j.quascirev.2011.09.001

Faul, K. L., Ravelo, A. C., & Delaney, M. L. (2000). Reconstructions of upwelling, productivity, and photic zone depth in the eastern equatorial pacific ocean using planktonic foraminiferal stable isotopes and abundances. *Journal of Foraminiferal Research*, *30*(2), 110–125. https://doi.org/10.2113/0300110

Fay, R. R. (1984). The goldfish ear codes the axis of acoustic particle motion in three dimensions. *Science*, *225*(4665), 951–954. https://doi.org/10.1126/science.6474161

Fernandez, A., Müller, I. A., Rodríguez-Sanz, L., van Dijk, J., Looser, N., & Bernasconi, S. M. (2017). A reassessment of the precision of carbonate clumped isotope measurements: Implications for calibrations and paleoclimate reconstructions. *Geochemistry, Geophysics, Geosystems*, *18*(12), 4375–4386. https://doi.org/10.1002/2017GC007106

Fosu, B. R., Ghosh, P., Mishra, D., Banerjee, Y., K, P., & Sarkar, A. (2019). Acid digestion of carbonates using break seal method for clumped isotope analysis. *Rapid Communications in Mass Spectrometry*, *33*(2), 203–214. https://doi.org/10.1002/rcm.8304

Fosu, B. R., Subba, R., Peethambaran, R., Bhattacharya, S. K., & Ghosh, P. (2020). Developments and applications in triple oxygen isotope analysis of carbonates. *ACS Earth and Space Chemistry*, *4*(5), 702–710. https://doi.org/10.1021/acsearthspacechem.9b00330

Froese, R., & Pauly, D. (2021). *Fishbase*. Retrieved from www.fishbase.org

Ghosh, P., Adkins, J., Affek, H., Balta, B., Guo, W., Schauble, E. A., et al. (2006). 13C–18O bonds in carbonate minerals: A new kind of paleothermometer. *Geochimica et Cosmochimica Acta*, *70*(6), 1439–1456. https://doi.org/10.1016/j.gca.2005.11.014

Ghosh, P., Eiler, J., Campana, S. E., & Feeney, R. F. (2007). Calibration of the carbonate 'clumped isotope' paleothermometer for otoliths. *Geochimica et Cosmochimica Acta*, *71*(11), 2736–2744. https://doi.org/10.1016/j.gca.2007.03.015

Gonfiantini, R., Stichler, W., & Rozanski, K. (1995). Standards and intercomparison materials distributed by the International Atomic Energy Agency for stable isotope measurements. In *Reference and intercomparison materials for stable isotopes of light elements* (pp. 13–29). International Atomic Energy Agency.

Gupta, A. K., Yuvaraja, A., Prakasam, M., Clemens, S. C., & Velu, A. (2015). Evolution of the South Asian monsoon wind system since the late Middle Miocene. *Palaeogeography, Palaeoclimatology, Palaeoecology*, *438*, 160–167. https://doi.org/10.1016/j.palaeo.2015.08.006

Hill, P. S., Schauble, E. A., & Tripati, A. (2020). Theoretical constraints on the effects of added cations on clumped, oxygen, and carbon isotope signatures of dissolved inorganic carbon species and minerals. *Geochimica et Cosmochimica Acta*, *269*, 496–539. https://doi.org/10.1016/j.gca.2019.10.016

Hill, P. S., Tripati, A. K., & Schauble, E. A. (2014). Theoretical constraints on the effects of pH, salinity, and temperature on clumped isotope signatures of dissolved inorganic carbon species and precipitating carbonate minerals. *Geochimica et Cosmochimica Acta*, *125*, 610–652. https://doi.org/10.1016/j.gca.2013.06.018

Huntington, K. W., Eiler, J. M., Affek, H. P., Guo, W., Bonifacie, M., Yeung, L. Y., et al. (2009). Methods and limitations of 'clumped' CO_2 isotope (Δ_{47}) analysis by gas-source isotope ratio mass spectrometry. *Journal of Mass Spectrometry*, *44*(9), 1318–1329. https://doi.org/10.1002/jms.1614

Jacob, K., & Sastri, V. V. (1952). Miocene foraminifera from Chavara, near Quilon in Travancore. *Records of the Geological Survey of India*, *82*(2), 342–353.

Jautzy, J. J., Savard, M. M., Dhillon, R. S., Bernasconi, S. M., & Smirnoff, A. (2020). Clumped isotope temperature calibration for calcite: Bridging theory and experimentation. *Geochemical Perspectives Letters*, *14*, 36–41. https://doi.org/10.7185/geochemlet.2021

John, C. M., & Bowen, D. (2016). Community software for challenging isotope analysis: First applications of 'Easotope' to clumped isotopes. *Rapid Communications in Mass Spectrometry*, *30*(21), 2285–2300. https://doi.org/10.1002/rcm.7720

Kalish, J. M. (1991a). ¹³C and ¹⁸O isotopic disequilibria in fish otoliths: Metabolic and kinetic effects. *Marine Ecology Progress Series*, *75*(2–3), 191–203. https://doi.org/10.3354/meps075191

Kalish, J. M. (1991b). Oxygen and carbon stable isotopes in the otoliths of wild and laboratory-reared Australian salmon (*Arripis trutta*). *Marine Biology*, *110*(1), 37–47. https://doi.org/10.1007/bf01313090

Kapur, V. V., Khosla, A., & Tiwari, N. (2019). Paleoenvironmental and paleobiogeographical implications of the microfossil assemblage from the Late Cretaceous intertrappean beds of the Manawar area, District Dhar, Madhya Pradesh, Central India. *Historical Biology*, *39*(1), 1145–1160. https://doi.org/10.1080/08912963.2018.1425408

Kelson, J. R., Huntington, K. W., Schauer, A. J., Saenger, C., & Lechler, A. R. (2017). Toward a universal carbonate clumped isotope calibration: Diverse synthesis and preparatory methods suggest a single temperature relationship. *Geochimica et Cosmochimica Acta*, *197*, 104–131. https://doi.org/10.1016/j.gca.2016.10.010

Kimball, J., Eagle, R., & Dunbar, R. (2016). Carbonate "clumped" isotope signatures in aragonitic scleractinian and calcitic gorgonian deep-sea corals. *Biogeosciences*, *13*(23), 6487–6505. https://doi.org/10.5194/bg-13-6487-2016

Lee, J. Y., Marotzke, J., Bala, G., Cao, L., Corti, S., Dunne, J. P., et al. (2021). Future global climate: Scenario-based projections and near-term information. In P. Z. V. Masson-Delmotte, A. Pirani, S. L. Connors, C. Péan, S. Berger, et al. (Eds.), *Climate change 2021: The physical science basis. Contribution of working group I to the sixth assessment report of the intergovernmental panel on climate change*. Cambridge University Press.

Martin, T. J., & Heemstra, P. C. (2015). Identification of Ambassis species (Pisces: Perciformes, Ambassidae) from South Africa. *South African Journal of Zoology*, *23*(1), 7–12. https://doi.org/10.1080/02541858.1988.11448070

Meckler, A. N., Ziegler, M., Millán, M. I., Breitenbach, S. F. M., & Bernasconi, S. M. (2014). Long-term performance of the Kiel carbonate device with a new correction scheme for clumped isotope measurements. *Rapid Communications in Mass Spectrometry*, *28*(15), 1705–1715. https://doi.org/10.1002/rcm.6949

Morris, R. W., & Kittleman, L. R. (1967). Piezoelectric property of otoliths. *Science*, *158*(3799), 368–370. https://doi.org/10.1126/science.158.3799.368

Müller, P., Staudigel, P. T., Murray, S. T., Vernet, R., Barusseau, J.-P., Westphal, H., & Swart, P. K. (2017). Prehistoric cooking versus accurate palaeotemperature records in shell midden constituents. *Scientific Reports*, *7*(1), 3555. https://doi.org/10.1038/s41598-017-03715-8

Narayanan, V., Anirudhan, S., & Grottoli, A. (2007). Oxygen and carbon isotope analysis of the Miocene limestone of Kerala and its implications to palaeoclimate and its depositional setting. *Current Science*, *93*, 1155–1159.

Patterson, W. P., Smith, G. R., & Lohmann, K. C. (2013). Continental paleothermometry and seasonality using the isotopic composition of aragonitic otoliths of freshwater fishes. In *Climate change in continental isotopic records* (pp. 191–202). American Geophysical Union (AGU). https://doi.org/10.1029/GM078p0191

Peeters, F. J. C., Brummer, G.-J. A., & Ganssen, G. (2002). The effect of upwelling on the distribution and stable isotope composition of *Globigerina bulloides* and *Globigerinoides ruber* (planktic foraminifera) in modern surface waters of the NW Arabian Sea. *Global and Planetary Change*, *34*(3), 269–291. https://doi.org/10.1016/S0921-8181(02)00120-0

Petersen, S. V., Defliese, W. F., Saenger, C., Daëron, M., Huntington, K. W., John, C. M., et al. (2019). Effects of improved ¹⁷O correction on interlaboratory agreement in clumped isotope calibrations, estimates of mineral-specific offsets, and temperature dependence of acid digestion fractionation. *Geochemistry, Geophysics, Geosystems*, *20*(7), 3495–3519. https://doi.org/10.1029/2018GC008127

Pingitore, N. E. (1976). Vadose and phreatic diagenesis; processes, products and their recognition in corals. *Journal of Sedimentary Research*, *46*(4), 985–1006. https://doi.org/10.1306/212F70B8-2B24-11D7-8648000102C1865D

Pramanik, C., Chatterjee, S., Fosu, B. R., & Ghosh, P. (2020). Isotopic fractionation during acid digestion of calcite: A combined ab initio quantum chemical simulation and experimental study. *Rapid Communications in Mass Spectrometry*, *34*(13), e8790.

Prasanna, K., Ghosh, P., Bhattacharya, S. K., Mohan, K., & Anilkumar, N. (2016). Isotopic disequilibrium in Globigerina bulloides and carbon isotope response to productivity increase in Southern Ocean. *Scientific Reports*, *6*(1), 21533. https://doi.org/10.1038/srep21533

Raha, P. K., Sinha Roy, S., & Rajendran, C. P. (1983). A new approach to lithostratigraphy of the Cenozoic sequence of Kerala. *Journal of the Geological Society of India*, *24*, 325–342.

Raju, D. S. N. (1978). Contribution to the Neogene stratigraphy of two areas of Kerala basin with special reference to Myogypsinidae. In D. A. Rasheed (Ed.), *Proceedings of the VII Indian colloquium on micropalaeontology and stratigraphy*. Department of Geology, University of Madras.

Rasheed, D. A., & Ramachandran, K. K. (1978). Foraminiferal biostratigraphy of the Quilon beds of Kerala, India. In *Proceedings of the VII Indian colloquium on micropalaeontology and stratigraphy*.

Reuter, M., Kern, A. K., Harzhauser, M., Kroh, A., & Piller, W. E. (2013). Global warming and South Indian monsoon rainfall-lessons from the Mid-Miocene. *Gondwana Research*, *23*(3), 1172–1177. https://doi.org/10.1016/j.gr.2012.07.015

Saenger, C. P., Schauer, A. J., Heitmann, E. O., Huntington, K. W., & Steig, E. J. (2021). How [17]O excess in clumped isotope reference-frame materials and ETH standards affects reconstructed temperature. *Chemical Geology*, *563*, 120059. https://doi.org/10.1016/j.chemgeo.2021.120059

Schauble, E. A., Ghosh, P., & Eiler, J. M. (2006). Preferential formation of [13]C–[18]O bonds in carbonate minerals, estimated using first-principles lattice dynamics. *Geochimica et Cosmochimica Acta*, *70*(10), 2510–2529. https://doi.org/10.1016/j.gca.2006.02.011

Schauer, A. J., Kelson, J., Saenger, C., & Huntington, K. W. (2016). Choice of [17]O correction affects clumped isotope (Δ_{47}) values of CO_2 measured with mass spectrometry. *Rapid Communications in Mass Spectrometry*, *30*(24), 2607–2616. https://doi.org/10.1002/rcm.7743

Sibony-Nevo, O., Pinkas, I., Farstey, V., Baron, H., Addadi, L., & Weiner, S. (2019). The Pteropod *Creseis acicula* forms its shell through a disordered nascent aragonite phase. *Crystal Growth & Design*, *19*(5), 2564–2573. https://doi.org/10.1021/acs.cgd.8b01400

Singh, A. D., Jung, S. J. A., Darling, K., Ganeshram, R., Ivanochko, T., & Kroon, D. (2011). Productivity collapses in the Arabian Sea during glacial cold phases. *Paleoceanography*, *26*(3). https://doi.org/10.1029/2009PA001923

Swart, P. K., Murray, S. T., Staudigel, P. T., & Hodell, D. A. (2019). Oxygen isotopic exchange between CO_2 and phosphoric acid: Implications for the measurement of clumped isotopes in carbonates. *Geochemistry, Geophysics, Geosystems*, *20*(7), 3730–3750. https://doi.org/10.1029/2019GC008209

Thiagarajan, N., Adkins, J., & Eiler, J. (2011). Carbonate clumped isotope thermometry of deep-sea corals and implications for vital effects. *Geochimica et Cosmochimica Acta*, *75*(16), 4416–4425. https://doi.org/10.1016/j.gca.2011.05.004

Thorrold, S. R., Campana, S. E., Jones, C. M., & Swart, P. K. (1997). Factors determining $\delta^{13}C$ and $\delta^{18}O$ fractionation in aragonitic otoliths of marine fish. *Geochimica et Cosmochimica Acta*, *61*(14), 2909–2919. https://doi.org/10.1016/S0016-7037(97)00141-5

Toffolo, M. B. (2021). The significance of aragonite in the interpretation of the microscopic archaeological record. *Geoarchaeology*, *36*(1), 149–169. https://doi.org/10.1002/gea.21816

Tripati, A. K., Roberts, C. D., & Eagle, R. A. (2009). Coupling of CO_2 and ice sheet stability over major climate transitions of the last 20 million years. *Science*, *326*(5958), 1394–1397. https://doi.org/10.1126/science.1178296

Upadhyay, D., Lucarelli, J., Arnold, A., Flores, R., Bricker, H., Ulrich, R. N., et al. (2021). Carbonate clumped isotope analysis (Δ_{47}) of 21 carbonate standards determined via gas-source isotope-ratio mass spectrometry on four instrumental configurations using carbonate-based standardization and multiyear data sets. *Rapid Communications in Mass Spectrometry*, *35*(17), e9143. https://doi.org/10.1002/rcm.9143

Wang, Y., Passey, B., Roy, R., Deng, T., Jiang, S., Hannold, C., et al. (2020). Clumped isotope thermometry of modern and fossil snail shells from the Himalayan-Tibetan Plateau: Implications for paleoclimate and paleoelevation reconstructions. *GSA Bulletin*. https://doi.org/10.1130/B35784.1

Weiner, S. (2010). *Microarchaeology: Beyond the visible archaeological record*. Cambridge University Press. https://doi.org/10.1017/CBO9780511811210

Willmes, M., Lewis, L. S., Davis, B. E., Loiselle, L., James, H. F., Denny, C., et al. (2019). Calibrating temperature reconstructions from fish otolith oxygen isotope analysis for California's critically endangered Delta Smelt. *Rapid Communications in Mass Spectrometry*, *33*(14), 1207–1220. https://doi.org/10.1002/rcm.8464

Wostbrock, J. A. G., Brand, U., Coplen, T. B., Swart, P. K., Carlson, S. J., Brearley, A. J., & Sharp, Z. D. (2020). Calibration of carbonate-water triple oxygen isotope fractionation: Seeing through diagenesis in ancient carbonates. *Geochimica et Cosmochimica Acta*, *288*, 369–388. https://doi.org/10.1016/j.gca.2020.07.045

Yang, X., Groeneveld, J., Jian, Z., Steinke, S., & Giosan, L. (2020). Middle Miocene intensification of South Asian monsoonal rainfall. *Paleoceanography and Paleoclimatology*, *35*(12), e2020PA003853. https://doi.org/10.1029/2020PA003853

You, Y. (2010). Climate-model evaluation of the contribution of sea-surface temperature and carbon dioxide to the Middle Miocene Climate Optimum as a possible analogue of future climate change. *Australian Journal of Earth Sciences*, *57*(2), 207–219. https://doi.org/10.1080/08120090903521671

You, Y., Huber, M., Müller, R. D., Poulsen, C. J., & Ribbe, J. (2009). Simulation of the middle Miocene climate optimum. *Geophysical Research Letters*, *36*(4). https://doi.org/10.1029/2008gl036571

Zachos, J., Pagani, M., Sloan, L., Thomas, E., & Billups, K. (2001). Trends, rhythms, and aberrations in global climate 65 Ma to present. *Science*, *292*(5517), 686–693. https://doi.org/10.1126/science.1059412

Zhuang, G., Pagani, M., & Zhang, Y. G. (2017). Monsoonal upwelling in the western Arabian Sea since the middle Miocene. *Geology*, *45*(7), 655–658. https://doi.org/10.1130/g39013.1